Guanine Residues in d(T_2AG_3) and d(T_2G_4) Form Parallel-Stranded Potassium Cation Stabilized G-Quadruplexes with Anti Glycosidic Torsion Angles in Solution†

Yong Wang‡ and Dinshaw J. Patel*,‡,§

Department of Biochemistry and Molecular Biophysics, College of Physicians and Surgeons, Columbia University, New York, New York 10032, and Program in Cellular Biochemistry and Biophysics, Rockefeller Research Laboratories, Memorial Sloan-Kettering Cancer Center, New York, New York 10021

Received April 27, 1992

ABSTRACT: We report below on proton NMR studies of the G-quadruplex structure formed by the human telomere sequence d(T_2AG_3) and the tetrahymena telomere sequence d(T_2G_4) in K cation containing solution. We observe well-resolved proton NMR spectra corresponding to a G-quadruplex monomer conformation predominant at 50 mM K cation concentration and a G-quadruplex dimer conformation predominant at 300 mM K cation concentration. By contrast, d(T_2AG_3T) and d(T_2G_4T) form only the G-quadruplex monomer structures independent of K cation concentration as reported previously [Sen, D., & Gilbert, W. (1992) *Biochemistry 31*, 65–70]. We detect well-resolved resonances for the exchangeable guanine imino and amino protons involved in G-tetrad formation with the hydrogen-bonded and exposed amino protons separated by up to 3.5 ppm. The observed NOEs between the amino and H8 protons on adjacent guanines within individual G-tetrads support the Hoogsteen pairing alignment around the tetrad. The imino protons of the internal G-tetrads exchange very slowly with solvent H_2O in the d(T_2AG_3) and d(T_2G_4) quadruplexes. The nature and intensity of the observed NOE patterns establish formation of parallel-stranded right-handed G-quadruplexes with all anti guanine glycosidic torsion angles. A model for the parallel-stranded G-quadruplex is proposed which is consistent with the experimental NOE data on the d(T_2AG_3) and d(T_2G_4) quadruplexes in solution. These results are in contrast to earlier studies on d($G_nT_mG_n$) sequences where the structures of the monovalent cation stabilized G-quadruplex exhibit alternating G(syn)–G(anti) glycosidic torsion angles along individual strands in solution [Wang, Y., de los Santos, C., Gao, X., Greene, K., Live, D., & Patel, D. J. (1991) *J. Mol. Biol. 222*, 819–832] and in the crystalline state [Kang, C. H., Zhang, X., Ratliff, R., Moyzis, R., & Rich, A. (1992) *Nature 356*, 126–131].

Guanine bases in DNA are unique in that they can align in a planar G-tetrad arrangement (structure **1**) stabilized

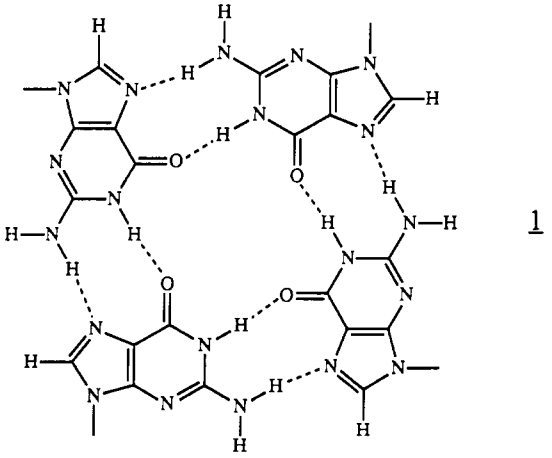

1

through Hoogsteen pairing in the presence of monovalent cations [reviewed in Guschlbauer et al. (1990), Sundquist (1991), and Sen and Gilbert (1991)]. Such G-tetrad pairing alignments have been observed and characterized in systems ranging from guanine monophosphates (Pinnavaia et al., 1975; Borzo et al., 1980) to poly(guanylic acid) (Gellert et al., 1962). Further, the role of monovalent cations in stabilizing G-quadruplexes has been systematically investigated (Howard & Miles, 1982; Lee et al., 1990). X-ray diffraction data on oriented, partially crystalline fibers of poly(guanylic acid) have been analyzed and interpreted in terms of a four-stranded right-handed helix with guanine bases paired in a G-tetrad alignment (Arnott et al., 1974; Zimmerman et al., 1975).

These early observations were not followed up until interest turned to the higher order structures adopted by single-stranded telomeric overhangs at the ends of chromosomes [reviewed in Blackburn and Szostak (1984) and Blackburn (1991)]. These include the d(T_2G_4), d(T_4G_4), and d(T_2AG_3) repeats observed in tetrahymena, oxytrichia, and human telomeres, respectively. The G-quadruplexes formed by such guanine-rich motifs could either adopt parallel-stranded structures will all anti guanine glycosidic torsion angles around the G-tetrad (Sen & Gilbert, 1988) or adopt antiparallel-stranded structures with alternating syn and anti guanine glycosidic torsion angles around the G-tetrad (Williamson et al., 1989; Sundquist & Klug, 1989; Panyutin et al., 1990). It was also established from footprinting and cross-linking studies on d($G_nN_mG_n$) segments that G-quadruplexes could form through pairing of four separate strands (Sen & Gilbert, 1988) or through dimerization of hairpins (Williamson et al., 1989; Sundquist & Klug, 1989; Panyutin et al., 1990). Further, it was proposed that these two families of structures could in-

† This research was supported by NIH Grant GM34504. The NMR spectrometers were purchased from funds donated by the Robert Woods Johnson Trust toward setting up an NMR Center in the Basic Medical Sciences at Columbia University.

* Address correspondence to this author.
‡ Columbia University.
§ Memorial Sloan-Kettering Cancer Center.

0006-2960/92/0431-8112$03.00/0

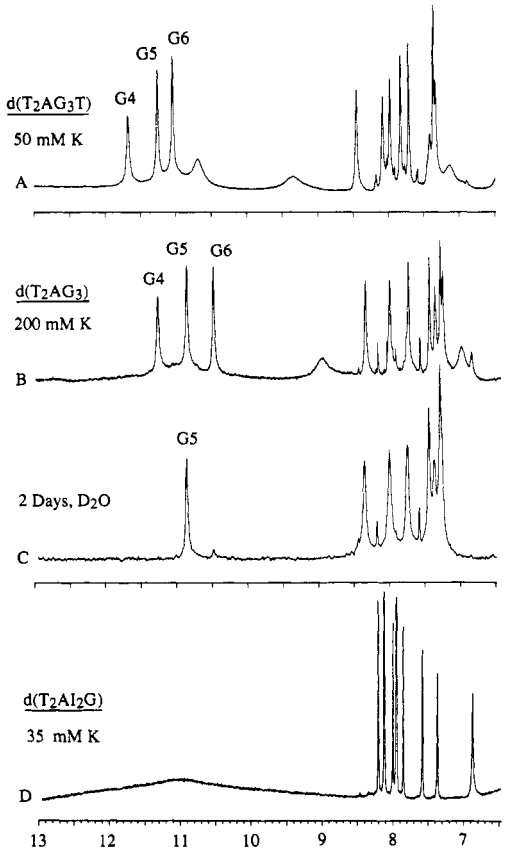

FIGURE 1: Proton NMR spectra (6.5–13.0 ppm) of (A) the d(T_2AG_3T) quadruplex in 50 mM K cation in H_2O at 5 °C, (B) the d(T_2AG_3) quadruplex in 200 mM K cation in H_2O at 8 °C, (C) the d(T_2AG_3) quadruplex in 200 mM K cation at 5 °C after being allowed to sit in D_2O for 2 days, and (D) the d(T_2AI_2G) quadruplex in 35 mM K cation in H_2O at 7 °C. All spectra were recorded at approximately neutral pH. The guanine imino proton assignments are recorded above the spectra. The narrow minor nonexchangeable resonances (7.0–8.5 ppm) correspond to protons from single-stranded structures in equilibrium with the quadruplex at this temperature.

terconvert, depending on the nature of the monovalent cation (Na or K) stabilizing the G-quadruplex structure (Sen & Gilbert, 1990; Hardin et al., 1992).

The conformations and thermodynamics of monovalent cation stabilized structures formed by d($G_nT_mG_n$) and d($G_nT_mG_nT_mG_nT_mG_n$) segments have been investigated by footprinting (Williamson et al., 1989), NMR (Henderson et al., 1987; Wang et al., 1991a,b; Smith & Feigon, 1992), calorimetric (Jin et al., 1990), spectroscopic (Hardin et al., 1991) and base analog substitution (Henderson et al., 1990) studies in solution and X-ray studies (Kang et al., 1992) in the crystalline state. The early NMR studies established that some guanines adopt syn glycosidic torsion angles (Henderson et al., 1987) and, more recently, that adjacent guanines alternate between syn and anti glycosidic torsion angles along individual strands (Wang et al., 1991a,b; Smith & Feigon, 1992) in solution. The directionality of individual strands and the differentiation between four-stranded and hairpin dimer structures for the d($G_nN_mG_n$) quadruplexes could not be differentiated from the available NMR data (Wang et al., 1991a,b) but could be defined on the basis of the X-ray structure of the d($G_4T_4G_4$) structure at atomic resolution (Kang et al., 1992). The crystallographic study established a G(syn)·G(anti)·G(syn)·G(anti) alignment around the G-tetrad. Adjacent guanines along individual strands alternate between syn and anti glycosidic torsion angles with overlaps differing between G(syn)–G(anti) and G(anti)–G(syn) steps.

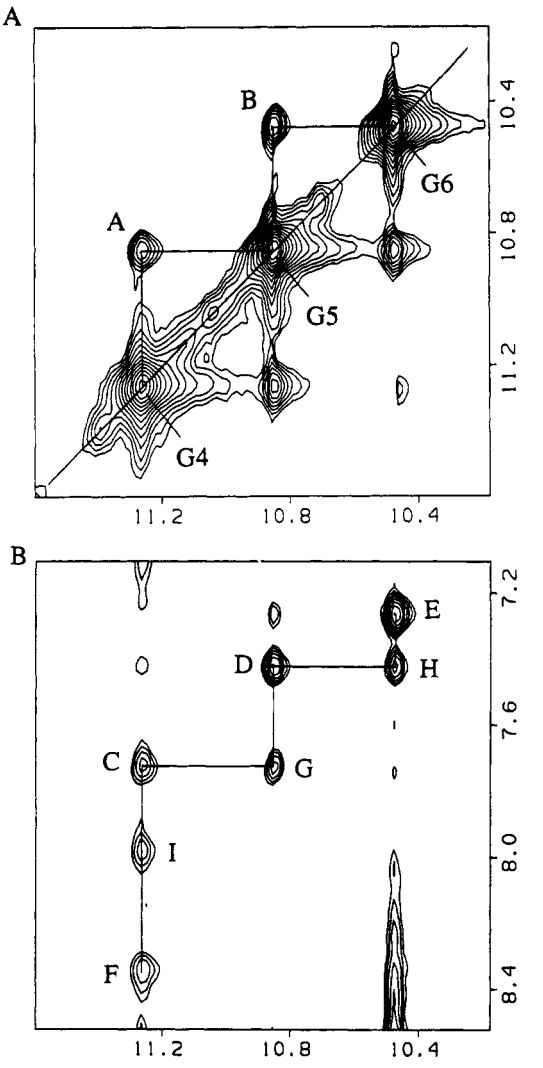

FIGURE 2: Expanded NOESY contour plot (mixing time 170 ms) of the d(T_2AG_3) quadruplex in 200 mM K cation in H_2O, neutral pH, at 5 °C. (A) Expanded symmetrical 10.2–11.6 ppm region. Cross peaks A and B are assigned as follows: A, G4(NH1)–G5(NH1); B, G5(NH1)–G6(NH1). (B) Expanded 10.2–11.6 and 7.0–8.6 ppm regions. Cross peaks C–I are assigned as follows: C, G4(NH1)–G4(H8); D, G5(NH1)–G5(H8); E, G6(NH1)–G6(H8); F, G4(NH1)–A3(H8); G, G5(NH1)–G4(H8); H, G6(NH1)–G5(H8); I, G4(NH1)–A3(H2).

Further, adjacent strands in the G-quadruplex are aligned in an antiparallel manner with the T_4 segments of d($G_4T_4G_4$) forming hairpin loops at either end. The X-ray structure identified a K cation sandwiched between the central G-tetrads accounting for the observed monovalent cation requirement for G-quadruplex formation. This X-ray structure (Kang et al., 1992) has provided an atomic resolution view of a G-quadruplex with antiparallel alignment of strands for G_4 motifs separated by a T_4 linker.

By contrast, structural information (either solution NMR or single-crystal X-ray) is lacking for parallel-stranded G-quadruplexes. Considerable experimental data including footprinting, strand mixing, and cross-linking studies have established that single multi-guanine motifs do form parallel-stranded G-quadruplexes for both dG_n (Sen & Gilbert, 1988, 1992; Lu et al., 1992) and rG_n (Kim et al., 1991) segments. We report below on NMR studies on the single repeat of the human telomere d(T_2AG_3) and the tetrahymena telomere d(T_2G_4) in K cation containing solution that address the issue of the structure of the metal cation stabilized parallel-stranded G-quadruplexes in solution. We have also monitored the K

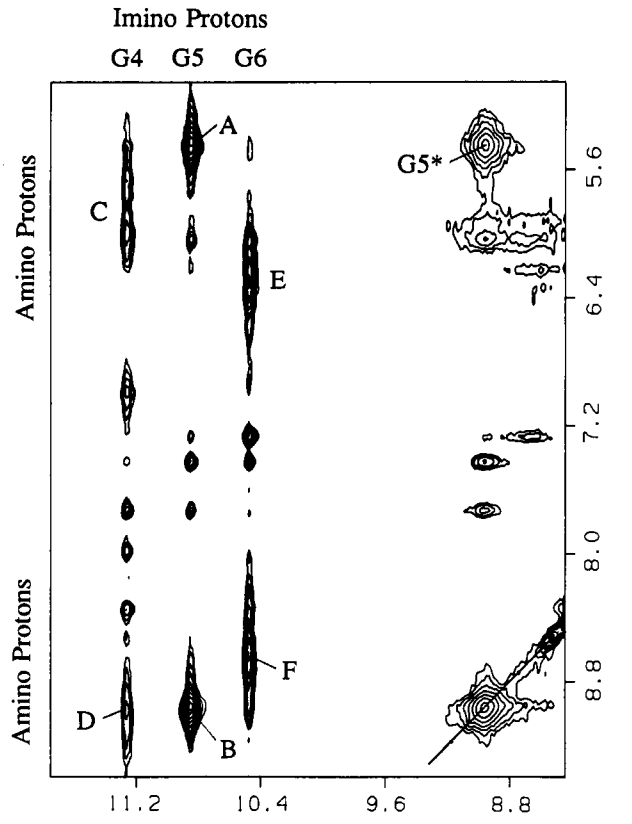

FIGURE 3: Expanded NOESY contour plot (mixing time 170 ms) of the $d(T_2AG_3)$ quadruplex in 200 mM K cation in H_2O, neutral pH, at 5 °C correlating the 8.6–11.6 ppm region with the 5.2–9.4 ppm region. Cross peaks A–F and G5* are assigned as follows: A, G5(NH1)–G5(NH2e); B, G5(NH1)–G5(NH2b); C, G4(NH1)–G4(NH2e); D, G4(NH1)–G4(NH2b); E, G6(NH1)–G6(NH2e); F, G6(NH1)–G6(NH2b); G5*, G5(NH_2b)–G5(NH_2e). Symbols b and e designate hydrogen-bonded and exposed guanine amino protons, respectively.

cation concentration-dependent transition between G-quadruplex monomer and dimer structures reported previously (Sen & Gilbert, 1992).

MATERIALS AND METHODS

Oligonucleotide Synthesis. The deoxyoligonucleotides were synthesized on an Applied Biosystems 391 DNA synthesizer using the solid-phase cyanoethyl phosphoramidite method. The crude 5′-dimethoxytritylated oligonucleotides were isolated by treatment of the support with concentrated ammonia for 15 h at 55 °C. The products were purified by reverse-phase HPLC. The 5′-dimethoxytrityl group was removed by treating the product with 80% acetic acid for 30 min followed by a second HPLC. The oligonucleotide products were desalted on a Sephadex G-25 column. The final sodium form of the oligonucleotides was obtained by using a Dowex 50X8 cation-exchange column.

NMR Experiments. DNA samples of 200–400 A_{260} units were dissolved in 0.4 mL of 90% H_2O/10% D_2O, and appropriate buffer and salt (i.e., KH_2PO_4 and KCl) were added to the desired concentrations. Two-dimensional phase-sensitive NOESY experiments (mixing time 170 ms) in H_2O were recorded on Bruker AM 500 and Bruker AM 400 spectrometers with the H_2O signal suppressed by a jump-and-return pulse sequence as the reading pulse. The carrier frequency was placed on the H_2O resonance with the maximum excitation centered at 11.4 ppm. Proton exchange was monitored by dissolving in D_2O the samples that had been lyophilized from H_2O. One-dimensional spectra were recorded immediately and over a matter of days thereafter. NOESY experiments in D_2O (mixing times 250 and 50 ms) were recorded with a sweep width of 9.6 ppm and a repetition delay of 1.5 s. The residual HDO signal was saturated using the decoupling channel. All data sets were transferred to a VAX 11-780 computer and processed with the FTNMR program provided by Dr. Dennis Hare (Hare Research). The spectra were collected with 1024 complex points in the t_2 dimension and 256 complex free induction decays in the t_1 dimension. The free induction decays were multiplied by a 90°-shifted sine-bell function zeroed to the 1024th point in the t_2 dimension and to the 256th point in the t_1 dimension.

Molecular Modeling. The model building was carried out on a Silicon Graphics IRIS-4D graphics workstation. A single B-form deoxynucleotide, dG, was first generated using the INSIGHT II program, version 2.1.0 (Biosym Technologies, Inc.). Four dG residues with anti glycosidic torsion angles and C2′-endo sugar pucker were aligned in a plane to form a G-tetrad. Four such G-tetrad planes were aligned on top of each other with a standard B-DNA rise (3.4 Å) and twist (36°). The bonds between P and O3′ atoms of the backbones were then linked. This four-stranded $d(G_4)$ quadruplex containing parallel strands and anti guanine glycosidic torsion angles was minimized without restraints for 500 iterations using the steepest descents method in the DISCOVER program, version 2.8.0 (Biosym Technologies, Inc.).

RESULTS

Exchangeable Protons in the $d(T_2AG_3)$ Quadruplex. The proton NMR spectrum (6.5–12.5 ppm) of $d(T_2AG_3)$ in 200 mM K cation in H_2O, neutral pH, at 8 °C is plotted in Figure 1B. Three exchangeable imino protons are detected between 10.4 and 11.3 ppm and exchangeable amino protons are detected at 9.0 and 7.0 ppm while the nonexchangeable base protons resonate between 7.0 and 8.5 ppm. The corresponding NMR spectrum taken 2 days after the sample was dissolved in D_2O is plotted in Figure 1C and shows that the imino proton at 10.85 ppm exchanges very slowly with solvent water. The imino protons observed between 10.4 and 11.3 ppm (Figure 1B) are characteristic of quadruplex formation (Wang et al., 1991a,b) for $d(T_2AG_3)$ in K cation containing solution. Consistent with this conclusion is the absence of imino protons in the same spectral region for $d(T_2AI_2G)$ in K cation containing solution (Figure 1D). The inosines in $d(T_2AI_2G)$ destabilize quadruplex formation as shown previously in another sequence context (Wang et al., 1981a).

Minor narrow resonances are detected between 7.0 and 8.0 ppm in the $d(T_2AG_3)$ NMR spectrum at low temperature (Figure 1B) and correspond to nonexchangeable protons of the single-stranded component in slow equilibrium with the quadruplex structure. The equilibrium shifts toward the single-stranded component when the temperature is increased.

Expanded NOESY contour plots of $d(T_2AG_3)$ in 200 mM K cation containing H_2O solution, neutral pH, at 5 °C recorded at a mixing time of 170 ms are plotted in Figure 2, panels A (symmetrical 10.0–11.6 ppm) and B (10.0–11.6 and 7.2–8.8 ppm). We detect NOEs between adjacent imino protons in the G4-G5-G6 segment of the d(T1-T2-A3-G4-G5-G6) quadruplex (cross peaks A and B, Figure 2A). Further, the guanine imino protons also exhibit NOEs to their own (cross peaks C–E, Figure 2B) and to their 5′-flanking (cross peaks F–H, Figure 2B) base H8 protons in the A3-G4-G5-G6 segment of the $d(T_2AG_3)$ quadruplex.

A different expanded region (8.6–11.6 and 5.2–9.4 ppm) of the same NOESY contour plot of $d(T_2AG_3)$ in 200 mM

Table I: Proton Chemical Shifts (ppm) of d(T-T-A-G-G-G) at pH 6.7[a]

	NH1	H2/NH$_2$-2	H8/H6	CH$_3$	H1′	H2′, H2″	H3′	H4′
T1			7.35	1.62	5.93	2.03, 2.28	4.59	3.94
T2			7.25	1.70	6.15	1.98, 2.27	4.67	4.01
A3		8.00	8.33		6.20	2.77, 2.86	5.02	4.39
G4	11.26		7.72		5.97	2.53, 2.84	4.93	4.46
G5	10.85	8.96, 5.45	7.44		6.04	2.65, 2.82	4.99	4.42
G6	10.48	8.64, 6.26	7.29		6.07	2.78, 2.56	4.81	4.26

[a] Exchangeable protons at 5 °C and nonexchangeable protons at 25 °C.

K cation in H_2O at 5 °C is plotted in Figure 3. The 10.85 ppm imino proton of G5 exhibits NOEs to its own amino protons at 8.96 and 5.45 ppm (cross peaks A and B, Figure 3). Further, the amino protons exhibit an NOE to each other (cross peak G5*, Figure 3). This unusually large 3.5 ppm separation between guanine amino protons is consistent with one of them forming a hydrogen bond while the other is exposed to solvent. The amino protons of G4 (cross peaks C and D, Figure 3) and G6 (cross peaks E and F, Figure 3) are broad, and the assignments in Figure 3 must be considered tentative at this time.

The exchangeable imino and amino proton chemical shifts for the d(T_2AG_3) quadruplex in 200 mM K cation at 5 °C are tabulated in Table I.

Nonexchangeable Protons in the d(T_2AG_3) Quadruplex. Expanded NOESY contour plots (mixing time 250 ms) are shown for the symmetrical base proton (7.0–8.6 ppm) region (Figure 4A), as well as between the base protons and the sugar H1′ protons (Figure 4B), the sugar H3′ protons (Figure 4C), and the sugar H2′,2″ protons (Figure 4D) of the d(T_2AG_3) quadruplex in 200 mM K cation containing D_2O solution, neutral pH, at 25 °C. We detect weak NOEs between adjacent H8 protons in the A3-G4-G5-G6 segment of the d(T_2AG_3) quadruplex (cross peaks A–C, Figure 4A).

We can trace the chain from T1 to G6 by monitoring the distance connectivities between the base protons and their own and 5′-flanking sugar H1′ protons in the d(T_2AG_3) quadruplex as shown in Figure 4B. The NOEs between the base and their own sugar H1′ protons for the guanine residues (cross peaks labeled G4, G5, and G6, Figure 4B) exhibit intensities which are similar to those observed for the same connectivity for the other base residues (cross peaks T1, T2, and A3, Figure 4B). The NOE cross peaks labeled G4, G5, and G6 (Figure 4B) exhibit weaker intensities than the NOEs between the H6 and CH_3 protons of T1 and T2 (cross peaks labeled T1* and T2*, Figure 4D; fixed interproton separation of 2.9 Å) in NOESY contour plots recorded at a short mixing time of 50 ms (data not shown). This observation establishes that guanines G4, G5, and G6 adopt anti glycosidic bond alignments (the separation between the H8 to its own H1′ proton is 3.7 Å for anti and 2.5 Å for syn glycosidic orientations) in the d(T_2AG_3) quadruplex in 200 mM K cation containing aqueous solution.

We can also trace the distance connectivities between the base protons and their own and 5′-flanking sugar H3′ protons in the d(T_2AG_3) quadruplex (Figure 4C). The base to their own sugar H3′ NOEs (labeled cross peaks in Figure 4C) are weak in the 50-ms mixing time NOESY data set (data not shown) and rule out a C3′-endo pucker for the sugars in the d(T_2AG_3) quadruplex (the separation between the base to its own H3′ proton is approximately 2.5 Å for a C3′-endo sugar pucker).

Finally, the base protons also exhibit NOEs to their own and 5′-flanking sugar H2′,2″ protons in the d(T_2AG_3) quadruplex (Figure 4D). The observed directionality of the NOEs from the base to the 5′-flanking sugar but not the 3′-flanking sugar H1′, H2′,2″, and H3′ protons establishes that the individual strands of the quadruplex adopt a right-handed helical alignment.

The nonexchangeable base and sugar proton chemical shifts for the d(T_2AG_3) quadruplex in 200 mM K cation at 25 °C are tabulated in Table I.

d(T_2AG_3T) Quadruplex. The proton spectrum (6.5–12.5 ppm) of d(T_2AG_3T) in 50 mM K cation in H_2O, neutral pH, at 5 °C is plotted in Figure 1A. This sequence also forms a quadruplex based on the guanine imino protons detected between 10.9 and 11.8 ppm. The exchangeable and nonexchangeable protons of the d(T_2AG_3) quadruplex have been assigned from an analysis of NOESY data sets in H_2O and D_2O (data not shown), and their chemical shifts are listed in Table II. We note that the guanine imino protons shift upfield on proceeding from the d(T_2AG_3T) quadruplex (Figure 1A) to the d(T_2AG_3) quadruplex (Figure 1B).

d(T_2G_4) and d(T_2G_4T) Quadruplexes. The proton NMR spectra (6.5–12.5 ppm) of d(T_2G_4) in 50 mM K cation and 300 mM K cation containing H_2O, neutral pH, solution at low temperature are plotted in Figure 5, panels B and C, respectively. Four narrow imino proton resonances are detected between 10.2 and 11.7 ppm and have been assigned to specific guanines on the basis of an analysis of NOESY data sets. The guanine imino protons are assigned over the resonances and establish a predominant conformation for d(T_2G_4) in 50 mM K cation (Figure 5B) and another predominant conformation for d(T_2G_4) in 300 mM K cation (Figure 5C) solution. All four guanine imino protons of d(T_2G_4) shift upfield to different extents on proceeding from 50 mM K cation (Figure 5B) to 300 mM K cation (Figure 5C) containing solutions. The G4 and G5 imino protons of the d(T_2G_4) quadruplex at low and high K cation concentrations exchange very slowly since they are still observed 2 days after the sample was dissolved in D_2O solution. An example of this is shown for the 300 mM K cation containing sample of d(T_2G_4) in Figure 5D.

We also note that the guanine imino proton spectrum (10.8–11.6 ppm) of d(T_2G_4) in 50 mM K cation (Figure 5B) is very similar to that of d(T_2G_4T) (Figure 5A), with the latter spectrum being independent of K cation between 50 and 300 mM concentration.

An expanded NOESY contour plot (mixing time 170 ms) of d(T_2G_4) in 300 mM K cation containing H_2O solution, neutral pH, at 5 °C correlating NOEs between the 8.4–11.6 ppm region and the 5.5–10.0 ppm region is plotted in Figure 6. Each guanine imino proton exhibits NOE cross peaks to resolved hydrogen-bonded and exposed guanine amino protons in the d(T_2G_4) quadruplex (cross peaks A and B are assigned to G3, cross peaks C and D are assigned to G4, cross peaks E and F are assigned to G5, and cross peaks G and H are assigned to G6; Figure 6). The resolved hydrogen-bonded and exposed amino protons of each guanine are linked by a distinct NOE cross peak in the contour plot (cross peaks labeled

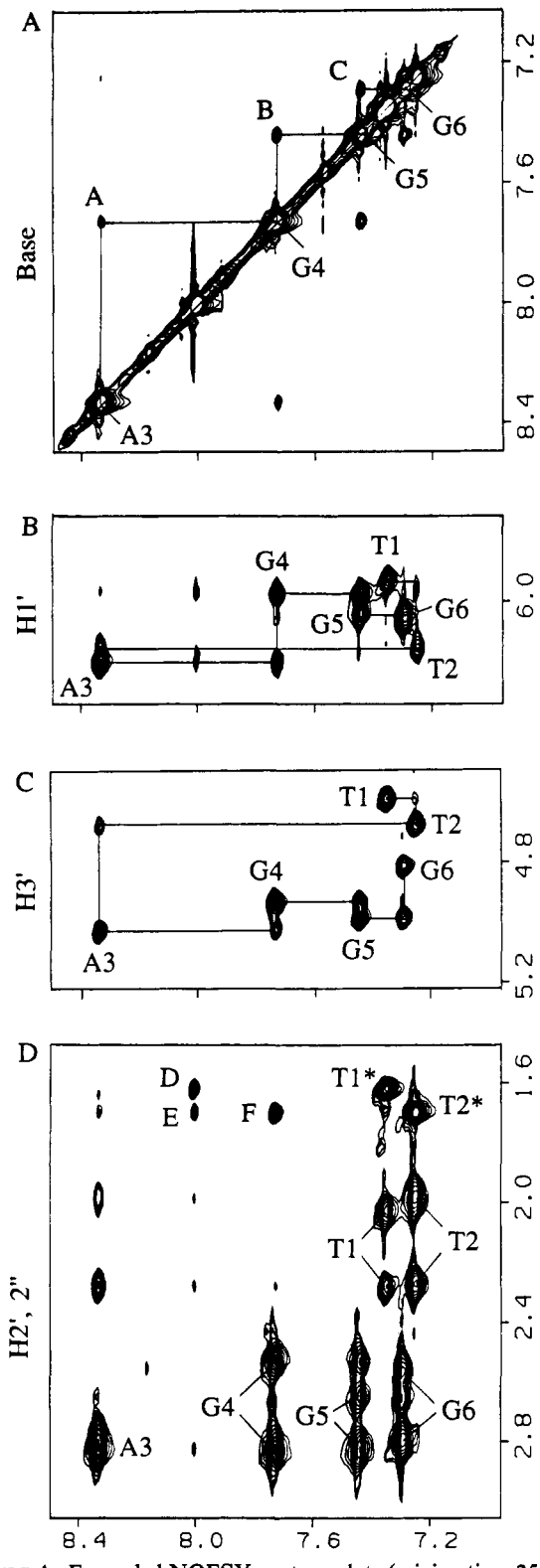

FIGURE 4: Expanded NOESY contour plots (mixing time 250 ms) of the $d(T_2AG_3)$ quadruplex in 200 mM K cation in D_2O, neutral pH, at 25 °C. (A) Expanded symmetrical 7.0–8.5 ppm region. Cross peaks A–C are assigned as follows: A, A3(H8)–G4(H8); B, G4(H8)–G5(H8); C, G5(H8)–G6(H8). (B) Expanded 7.0–8.5 and 5.8–6.4 ppm regions. The lines trace the NOEs between the base protons and their own and 5′-flanking sugar H1′ protons. The base to their own sugar H1′ NOEs are marked by residue position. (C) Expanded 7.0–8.5 and 4.4–5.1 ppm regions. The base to their own sugar H3′ NOEs are marked by residue position. (D) Expanded 7.0–8.5 and 1.4–3.0 ppm regions. The base to their own sugar H2′,2″ NOEs are marked by residue position. Cross peaks D–F and T1* and T2* are assigned as follows: D, A3(H2)–T1(CH_3-5); E, A3(H2)–T2(CH_3-5); F, G4(H8)–T2(CH_3-5); T1*, T1(H6)–T1(CH_3); T2*, T2(H6)–T2(CH_3).

G3*, G4*, G5*, and G6*, Figure 6). Further, for $d(T_2G_4)$ we also observe a directionality to the NOEs between adjacent residues in the G3-G4-G5-G6 segment in that the guanine imino protons exhibit NOEs to their own H8 protons (cross peaks J, L, N, and P, Figure 6) and the H8 protons of the 5′-flanking residues (cross peaks I, K, M, and O, Figure 6).

DISCUSSION

Parallel-Stranded G-Quadruplexes. The proton NMR spectra of both $d(T_2AG_3T)$ (Figure 1A) and $d(T_2G_4T)$ (Figure 5A) in K cation containing aqueous solution at low temperature are characteristic of a single predominant conformation in solution. This result establishes that the guanines from each strand in the quadruplex must align in register, forming three G-tetrads in the $d(T_2AG_3T)$ quadruplex and forming four G-tetrads in the $d(T_2G_4T)$ quadruplex. Further, we only observe NOEs between protons on adjacent guanines, which is consistent with a parallel alignment of strands in both G-quadruplexes (structure **2**). For instance, an antiparallel

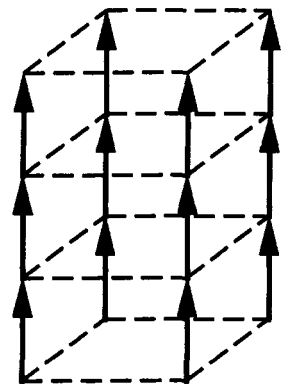

2

alignment of strands in the d(T-T-G3-G4-G5-G6-T) quadruplex would predict NOEs between the H8 and NH_2 protons on G3 and G6 which were not observed experimentally.

The observed NOEs between guanine H8 protons and their own and 5′-flanking sugar H1′, H2′,2″, and H3′ protons in the $d(T_2AG_3)$ quadruplex (Figure 4, panels B–D) establish that each strand adopts a right-handed alignment.

The magnitude of the NOEs between the guanine H8 and their own sugar H1′ protons at short mixing times requires that all guanines adopt an anti glycosidic bond alignment for the $d(T_2AG_3)$ and $d(T_2G_4)$ quadruplexes in K cation containing solution. Thus, the guanines must be anti along individual strands in these parallel-stranded G-quadruplexes. This contrasts strikingly with earlier observations of alternate G(syn)–G(anti) alignments along individual strands for $d(G_n)$ sequences separated by non-guanine linkers in $d(G_2N_5G_2)$ quadruplexes (Wang et al., 1991a,b) and $d(G_4T_4G_4)$ quadruplexes (Kang et al., 1992; Smith & Feigon, 1992). These quadruplexes are most likely generated by antiparallel alignment of hairpin dimers as rigorously established for $d(G_4T_4G_4)$ in the crystalline state (Kang et al., 1992).

G-Tetrad Alignment. A parallel-stranded G-quadruplex alignment requires that the same guanines from each of the four strands must align in a plane to form individual G-tetrads. An NOE is predicted between the amino protons and the H8 proton on adjacent Hoogsteen-paired guanines around individual G-tetrads (see **1**). These NOEs are observed experimentally (cross peaks Q, S, T, and U, Figure 6) as are the corresponding ones as a result of spin diffusion between the imino and the H8 protons around the G-tetrad (cross peaks J, L, N, and P, Figure 6) in the $d(T_2G_4)$ quadruplex.

Table II: Proton Chemical Shifts (ppm) of d(T-T-A-G-G-G-T) at pH 6.7[a]

	NH1	H2/NH$_2$-2	H8/H6	CH$_3$	H1′	H2′, H2″	H3′	H4′
T1			7.39	1.65	5.98	2.09, 2.32	4.63	3.98
T2			7.31	1.76	6.25	2.05, 2.33	4.72	4.04
A3		8.07	8.41		6.27	2.84, 2.90	5.08	4.43
G4	11.66		7.93		6.00	2.65, 2.90	5.03	4.48
G5	11.23	9.32, 6.11	7.77		6.02	2.64, 2.70	5.03	4.49
G6	11.02		7.69		6.25	2.55, 2.67	4.90	4.49
T7			7.34	1.60	6.05	2.17, 2.17	4.47	4.06

[a] Exchangeable protons at 5 °C and nonexchangeable protons at 25 °C.

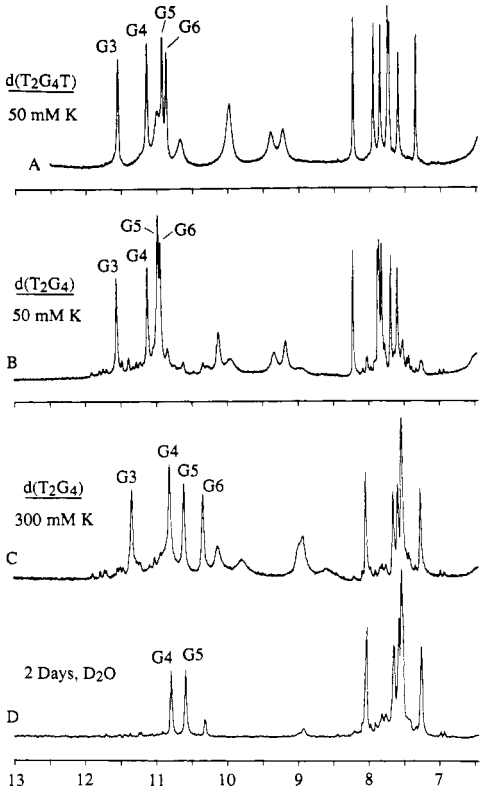

FIGURE 5: Proton NMR spectra (6.5–13.0 ppm) of (A) the d(T_2G_4T) quadruplex in 50 mM K cation in H_2O at 4 °C, (B) the d(T_2G_4) quadruplex in 50 mM K cation in H_2O at 3 °C, (C) the d(T_2G_4) quadruplex in 300 mM K cation in H_2O at 6 °C, and (D) the d(T_2G_4) quadruplex in 300 mM K cation at 5 °C after being allowed to sit in D_2O for 2 days. All spectra were recorded at approximately neutral pH. The guanine imino proton assignments are recorded above the spectra.

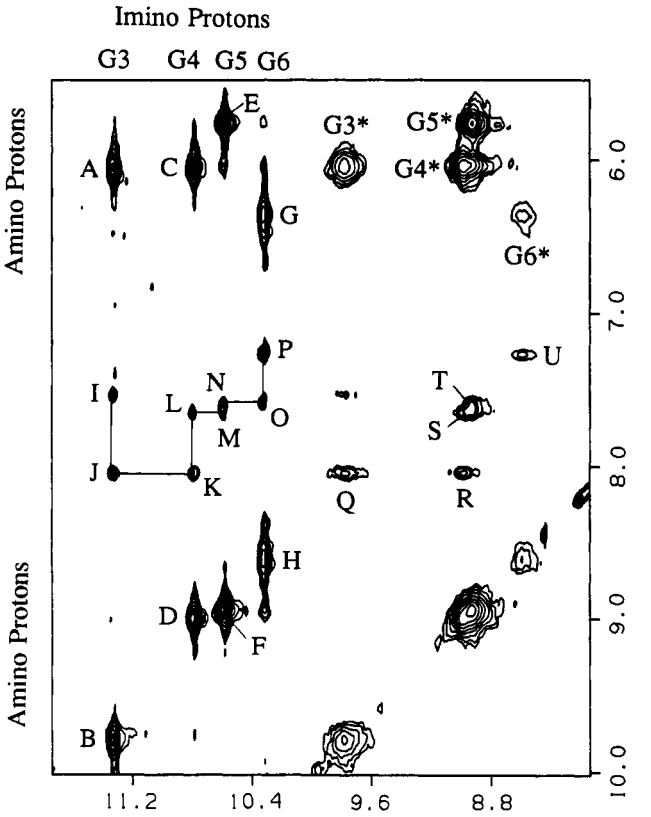

FIGURE 6: Expanded NOESY contour plot (mixing time 170 ms) of the d(T_2G_4) quadruplex in 300 mM K cation in H_2O, neutral pH, at 5 °C correlating the 8.4–11.6 ppm region with the 5.5–10.0 ppm region. Cross peaks A–H are assigned as follows: A, G3(NH1)–G3(NH2e); B, G3(NH1)–G3(NH2b); C, G4(NH1)–G4(NH2e); D, G4(NH1)–G4(NH2b); E, G5(NH1)–G5(NH2e); F, G5(NH1)–G5(NH2b); G, G6(NH1)–G6(NH2e); H, G6(NH1)–G6(NH2b). Cross peaks designated by asterisks are assigned as follows: G3*, G3(NH2b)–G3(NH2e); G4*, G4(NH2b)–G4(NH2e); G5*, G5(NH2b)–G5(NH2e); G6*, G6(NH2b)–G6(NH2e). Cross peaks I–P are assigned as follows: I, G3(NH1)–T2(H6); J, G3(NH1)–G3(H8); K, G4(NH1)–G3(H8); L, G4(NH1)–G4(H8); M, G5(NH1)–G4(H8); N, G5(NH1)–G5(H8); O, G6(NH1)–G5(H8); P, G6(NH1)–G6(H8). Cross peaks Q–U are assigned as follows: Q, G3(NH2b)–G3(H8); R, G4(NH2b)–G3(H8); S, G4(NH2b)–G4(H8); T, G5(NH2b)–G5(H8); U, G6(NH2b)–G6(H8). Symbols b and e designate hydrogen-bonded and exposed guanine amino protons, respectively.

The guanine N^1 imino protons are hydrogen-bonded to O^6 carbonyl groups in the Hoogsteen-pairing alignment of G-tetrads (see **1**). These guanine imino protons are centered about 11.0 ppm in the d(T_2AG_3) and d(T_2G_4) quadruplexes (Figures 1 and 5) with this chemical shift range similar to the chemical shift observed for guanine imino protons hydrogen-bonded to carbonyl groups in Wobble G·T pairs (Patel et al., 1982). Further, the internal G5 imino proton in the d(T_2AG_3) quadruplex (Figure 1C) and the internal G4 and G5 imino protons in the d(T_2G_4) quadruplex (Figure 5D) exchange very slowly. The guanine imino protons are both hydrogen-bonded and in the interior of the G-tetrad (see **1**) so that those located on the nonterminal stacked G-tetrads should be shielded from solvent, accounting for their very slow exchange in K cation stabilized G-quadruplexes. A similar slow exchange was observed for nonterminal guanine imino protons in the quadruplex structures formed by d($G_4T_4G_4$) and d($G_4T_4G_4T_4G_4T_4G_4$) in Na cation containing solution (Smith & Feigon, 1992).

We also observe well-resolved guanine amino protons separated by chemical shifts ranging between 2.5 and 3.5 ppm (Figures 3 and 6). The downfield-shifted amino protons which resonate about 9 ppm must be hydrogen-bonded while the upfield-shifted amino proton must be exposed to solvent. Indeed, the Hoogsteen-paired alignment has one of the two amino protons hydrogen-bonded to the N^7 of an adjacent guanine around the G-tetrad (see **1**).

The observation of only anti guanine glycosidic torsion angles in the d(T_2AG_3) and d(T_2G_4) quadruplexes requires G(anti)·G(anti)·G(anti)·G(anti) alignments around individual G-tetrads

in parallel-stranded G-quadruplexes. This contrasts with an alternating G(syn)·G(anti)·G(syn)·G(anti) alignment around individual G-tetrads in the antiparallel-stranded G-quadruplex formed by dimerization of a pair of $d(G_4T_4G_4)$ hairpins in the crystalline state (Kang et al., 1992).

We do not observe strong NOEs between the guanine H8 and their own sugar H3′ protons at short mixing times in the $d(T_2AG_3)$ and $d(T_2G_4)$ quadruplexes. This rules out C3′-endo sugar puckers at guanine residues with anti glycosidic torsion angles in parallel-stranded G-quadruplexes.

K Cation Dependent Dimerization of G-Quadruplexes. Our NMR studies establish that $d(T_2G_4)$ adopts one conformation in 50 mM K cation solution (Figure 5B) and another conformation defined by upfield chemical shifts of the guanine imino protons in 300 mM K cation solution (Figure 5C). Further, $d(T_2G_4T)$ adopts only a single conformation independent of K cation concentration (Figure 5A) which is similar to that observed by $d(T_2G_4)$ in low K cation containing solution (Figure 5B).

These results are most readily rationalized by identifying the $d(T_2G_4)$ conformation in 50 mM K cation solution (guanine imino and H8 proton line widths of 10.5 and 6.5 Hz, respectively) as a G-quadruplex monomer while the $d(T_2G_4)$ conformation in 300 mM K cation solution (guanine imino and H8 proton line widths of 16.5 and 9.5 Hz, respectively) as a dimer of G-quadruplexes. It is unlikely that the $d(T_2AG_3)$ and $d(T_2G_4)$ quadruplexes form simple back-to-back dimers since all the guanine imino protons shift upfield on proceeding from the monomer to the dimer.

Indeed, this phenomenon of K cation dependent formation of higher order alignments of G-quadruplexes containing a single multi-guanine motif at the 3′-end has been reported previously (Sen & Gilbert, 1992). This group proposed formation of front-to-back alignments of two G-quadruplexes containing G-tetrads formed by out-of-register guanines on the basis of methylation protection experiments.

Model of the Parallel-Stranded G-Quadruplex. We have generated a model of the G-quadruplex (see Materials and Methods) which satisfies the following constraints deduced from the structural NMR studies on the $d(T_2AG_3)$ and the $d(T_2G_4)$ family of quadruplexes: (1) The strands are parallel in the G-quadruplex and adopt a right-handed helical twist. (2) All guanines adopt an anti glycosidic torsion angle and the guanine sugars do not adopt a C3′-endo pucker. (e) The guanine imino proton and one amino proton are hydrogen-bonded around the G-tetrad and the pairing alignment is as shown in **1**.

A model of this right-handed parallel-stranded G-quadruplex containing four stacked G-tetrads is shown in Figure 7A. This view is slightly tilted from the normal to the helix axis and looks into one of the four equivalent grooves of the G-quadruplex. A view down the helix aixs identifying the guanine base overlaps between adjacent G-tetrads is shown in Figure 7B. There is partial overlap between the five- and six-membered rings of adjacent guanines on the same strand. The helix twist between adjacent G-tetrads is 30°, and there exists a hole down the helix axis. The model qualitatively explains the observed NOEs between base protons such as between adjacent guanine imino protons (distance 3.64 Å in the model) and adjacent guanine H8 protons (distance 5.0 Å in the model) on the same strand as well as between adjacent hydrogen-bonded guanine amino and guanine H8 protons (distance 3.36 Å in the model) around a G-tetrad. The model also explains the trend in the observed NOEs between the base protons and their own and 5′-flanking sugar protons on individual strands on the parallel-stranded G-quadruplex.

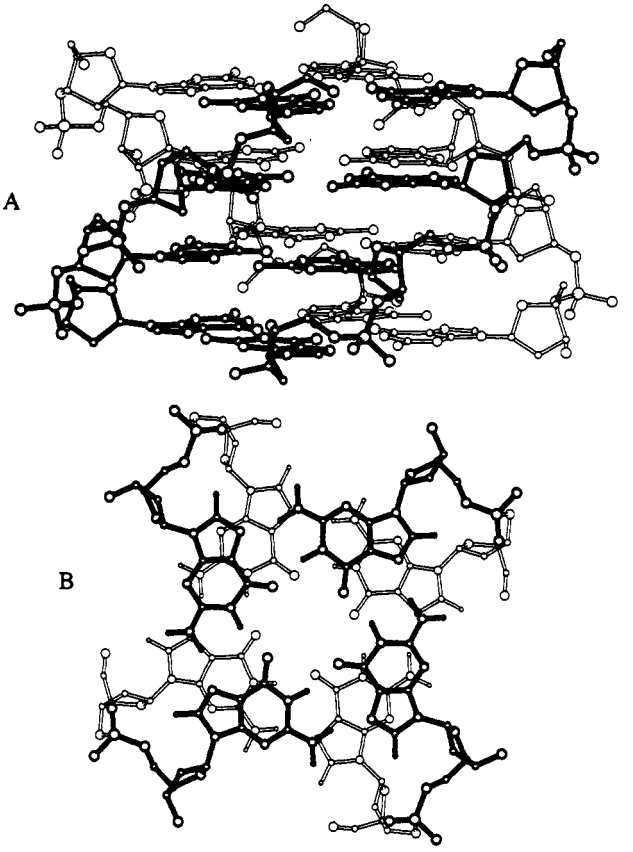

FIGURE 7: (A) Model of the right-handed parallel-stranded G-quadruplex containing four stacked G-tetrads (see Materials and Methods). This view is slightly tilted from the normal to the helix axis and looks into one of the four equivalent grooves of the G-quadruplex. The 5′-ends of individual strands are at the top and the 3′-ends at the bottom of the figure. (B) View down the helix axis of the model identifying the guanine base overlaps between adjacent G-tetrads. The helical twist between adjacent G-tetrads is 30°, and there exists a hole down the helix axis.

A more quantitative effort is underway to input the NMR-based experimental distance constraints deduced from NOE buildup curves in a molecular dynamics computation to define features of the solution structure of a parallel-stranded G-quadruplex. Such an analysis will include the back-calculation approach which minimizes the difference between experimental and calculated NOESY spectra.

Summary. Previous investigations (Sen & Gilbert, 1988, 1992) and the current NMR study establish that single multi-guanine motifs align through parallel orientations to form G-quadruplexes containing stacked G-tetrads with all anti guanine glycosidic torsion angles. The proton spectrum of the $d(T_2G_4T)$ in K cation containing solution (Figure 5A) demonstrates formation of a single conformation of the G-quadruplex monomer with well-resolved guanine imino (10.8–11.6 ppm), hydrogen-bonded amino (9.0–10.3 ppm), and H8 (7.3–8.3 ppm) protons. These assigned markers should be especially useful for monitoring the interaction of ligands with the four equivalent grooves of the parallel-stranded G-quadruplex structure in solution. We observe formation of monomer and dimer conformations of the $d(T_2G_4)$ quadruplex with this equilibrium modulated by the K cation concentration of the solution. This structural information on parallel-stranded G-quadruplexes in solution complements the recent X-ray structural characterization of an antiparallel-stranded G-quadruplex (Kang et al., 1992).

REFERENCES

Arnott, S., Chandrasekaran, R., & Martilla, C. M. (1974) *Biochem. J. 141*, 537–543.

Blackburn, E. H. (1991) *Nature 350*, 569–573.

Blackburn, E. H., & Szostak, J. W. (1984) *Annu. Rev. Biochem. 53*, 163–194.

Borzo, M., Detellier, C., Lazlo, P., & Paris, A. (1980) *J. Am. Chem. Soc. 102*, 1124–1134.

Gellert, M., Lipsett, M. N., & Davies, D. R. (1962) *Proc. Natl. Acad. Sci. U.S.A. 48*, 2013–2018.

Guschlbauer, W., Chantot, J. F., & Thiele, D. (1990) *J. Biomol. Struct. Dyn. 8*, 491–511.

Hardin, C. C., Henderson, E., Watson, T., & Prosser, J. K. (1991) *Biochemistry 30*, 4460–4472.

Hardin, C. C., Watson, T., Corregan, M., & Bailey, C. (1992) *Biochemistry 31*, 833–841.

Henderson, E. R., Hardin, C. C., Wolk, S. K., Tinoco, I., Jr., & Blackburn, E. H. (1987) *Cell 51*, 899–908.

Henderson, E. R., Moore, M., & Malcolm, B. A. (1990) *Biochemistry 29*, 732–737.

Howard, F. B., & Miles, H. T. (1982) *Biochemistry 21*, 6736–6745.

Jin, R., Breslauer, K. J., Jones, R. A., & Gaffney, B. L. (1990) *Science 250*, 543–546.

Kang, C. H., Zhang, X., Ratliff, R., Moyzis, R., & Rich, A. (1992) *Nature 356*, 126–131.

Kim, J., Cheong, C., & Moore, P. B. (1991) *Nature 351*, 331–332.

Lee, J. S. (1991) *Nucleic Acids Res. 18*, 6057–6060.

Lu, M., Guo, Q., & Kallenbach, N. R. (1992) *Biochemistry 31*, 2455–2459.

Panyutin, I. G., Kovalsky, O. I., Budowsky, E. I., Dickerson, R. E., Rikhirev, M. E., & Lipanov, A. A. (1990) *Proc. Natl. Acad. Sci. U.S.A. 87*, 867–870.

Patel, D. J., Kozlowski, S. A., Marky, L. A., Rice, J. A., Broka, C., Dallas, J., Itakura, K., & Breslauer, K. J. (1982) *Biochemistry 21*, 437–444.

Pinnavaia, T. J., Marshall, C. L., Mettler, C. M., Fisk, C. L., Miles, H. T., & Becker, E. D. (1978) *J. Am. Chem. Soc. 100*, 3625–3627.

Sen, D., & Gilbert, W. (1988) *Nature 334*, 364–366.

Sen, D., & Gilbert, W. (1990) *Nature 344*, 410–414.

Sen, D., & Gilbert, W. (1991) *Curr. Opin. Struct. Biol. 1*, 435–438.

Sen, D., & Gilbert, W. (1992) *Biochemistry 31*, 65–70.

Smith, F. W., & Feigon, J. (1992) *Nature 356*, 164–168.

Sundquist, W. I. (1991) in *Nucleic Acids in Molecular Biology* (Lilley, D. M., & Eckstein, F., Eds.) Springer-Verlag, New York.

Sundquist, W. I., & Klug, A. (1989) *Nature 342*, 825–829.

Wang, Y., de los Santos, C., Gao, X., Greene, K., Live, D., & Patel, D. J. (1991a) *J. Mol. Biol. 222*, 819–832.

Wang, Y., Jin, R., Gaffney, B., Jones, R. A., & Breslauer, K. J. (1991b) *Nucleic Acids Res. 19*, 4619–4622.

Williamson, J. R., Raghuraman, M. K., & Cech, T. R. (1989) *Cell 59*, 871–880.

Zimmerman, S. B., Cohen, G. H., & Davies, D. R. (1975) *J. Mol. Biol. 92*, 181–192.